ELSEVIER

Catalysis Today 66 (2001) 249–254

CATALYSIS TODAY

www.elsevier.com/locate/cattod

Mesoscale modeling in multiphase catalysis

František Štěpánek [a,b], Miloš Marek [a,*], Jiří Hanika [c], Pierre M. Adler [b]

[a] *Department of Chemical Engineering, Prague Institute of Chemical Technology, Technická 5, 166 28 Praha 6, Czech Republic*
[b] *Laboratoire Milieux Poreux et Fracturés, Institut de Physique du Globe de Paris, 4 place Jussieu, 75252 Paris Cedex 05, France*
[c] *Department of Organic Technology, Prague Institute of Chemical Technology, Technická 5, 166 28 Praha 6, Czech Republic*

Abstract

Methodology and software for pore-scale modeling of multi-phase heterogeneous catalytic reactions is described. Its main features include the modeling of internal wetting with simultaneous phase transition and chemical reaction, and the calculation of liquid- and vapor-phase distribution inside the pore space of a computer-reconstructed catalyst pellet or washcoat layer, under periodically varying external conditions.

Keywords: Porous media; Internal wetting; Capillary flow; Non-stationary operation; Hysteresis

1. Background and objectives

Both computer software and relatively well-established methodologies currently exist for the modeling of fixed-bed catalytic processed (both single- and multi-phase) at two different length-scales: the molecular scale (with the objective of predicting reactivity and phase equilibria using Molecular Dynamics [1]), and the reactor scale (simulation of momentum, heat, and mass transfer in packed beds, oriented packings, and monoliths by means of Computational Fluid Dynamics [2,3]). However, the efficiency with which physico-chemical properties of a catalytically active porous solid translate into process performance characteristics of a multi-phase reactor depend also on phenomena taking place inside individual pores of the catalyst carrier — on the "mesoscale".

The morphological characteristics of a porous structure determine its key transport properties such as the effective diffusivity, hydrodynamic permeability, and thermal conductivity [4], all of which are very important parameters for the design of multi-phase catalytic processes. Despite the importance of a detailed understanding of phenomena at the mesoscale, particle-level models used so far are relatively unsophisticated in comparison with their molecular- or reactor-level counterparts. They are mostly based on "effective medium" approaches which treat the porous solid as a pseudo-homogeneous material possessing certain volume-averaged transport properties. In multiphase catalysis, however, both liquid and vapor phase coexist within the pore space and since the transport mechanisms can be relatively complex [5], "local" heterogeneous models are required in order to describe all substantial phenomena such as hysteresis [6,7].

The objective of this contribution is to demonstrate methodology and computer code for the calculation of the distribution of liquid and vapor phases in the pore space of an arbitrary porous medium where capillary forces are the dominant mechanism of fluid transport. Such computer code forms the core of mesoscale modeling tools in multi-phase catalysis, as it enables the calculation of parameters such as the degree of internal wetting [8], which determines the reaction rate.

* Corresponding author. Tel.: +420-2-2435-3104; fax: +420-2-311-7335.
E-mail address: marek@tiger.vscht.cz (M. Marek).

0920-5861/01/$ – see front matter
PII: S0920-5861(00)00628-3

2. Problem formulation

Let us assume the following situation, inspired by the well-studied model case of cyclohexene hydrogenation over palladium on carbon [9]: a porous catalyst pellet or a washcoat layer (Fig. 1a and b) are subject to periodic external wetting [10], and a heterogeneously catalyzed irreversible reaction

$$\mathrm{E} + \mathrm{H} \rightarrow \mathrm{A} \tag{1}$$

takes place in its pore space. Under typical operating conditions (atmospheric pressure, temperature below the normal boiling points of A and E), the liquid-phase is a mixture of components E and A, with a small amount of absorbed component H, according to the Henry's law

$$x_{\mathrm{H}} = \frac{p_{\mathrm{H}}}{K_{\mathrm{H}}} \tag{2}$$

where x_{H} is the mole fraction of H in the liquid mixture, p_{H} (Pa) its partial pressure in the gas-phase, and K_{H} the Henry constant, which is calculated from the correlation $\ln(K_{\mathrm{H}}) = 11.56 + 548.68/T - 0.169\ln(T) - 0.001\,T$ (in kPa). The gas-phase is formed mainly by H, with equilibrium vapor pressures of A and E according to the Raoult's law

$$p_i = p_i^0(T)x_i, \quad i = \mathrm{E}, \mathrm{A} \tag{3}$$

where $p_i^0(T)$ is the equilibrium vapor pressure of a pure component i at temperature T; p_{E}^0 is calculated from the Antoine equation $\ln p_{\mathrm{E}}^0 = 9.2041 - 2813.5/(T - 49.98)$ and p_{A}^0 from the correlation $\ln(p_{\mathrm{A}}^0/40.7) = (-6.9601\,T_{\mathrm{r}} + 1.3133\,T_{\mathrm{r}}^{3/2} - 2.7568\,T_{\mathrm{r}}^3 - 2.4549\,T_{\mathrm{r}}^6)/(1 - T_{\mathrm{r}})$, where $T_{\mathrm{r}} = T/553.5$ is the reduced temperature, and pressures are given in bars. Chemical reaction can proceed both as gas–solid and liquid–solid, with generally different kinetic relationships. We adopt power-law kinetics with the values of apparent rate constants, activation energies and reaction orders for cyclohexene hydrogenation from [11].

$$r_{\mathrm{l}} = 0.0652 \exp\left(-\frac{2516}{T}\right) x_{\mathrm{E}}^{0.05} x_{\mathrm{H}}^{0.61} \tag{4a}$$

$$r_{\mathrm{g}} = 0.4697 \exp\left(-\frac{503.2}{T}\right) y_{\mathrm{E}}^{0.95} y_{\mathrm{H}}^{0.66} \left(\frac{P_{\mathrm{g}}}{P_0}\right)^{1.61} \tag{4b}$$

The reaction rates are in $\mathrm{mol\,g_{cat}^{-1}\,s^{-1}}$, $P_0 = 10^5$ Pa, and $y_i = p_i/P_{\mathrm{g}}$ are the mole fractions in the gas-phase. The overall reaction rate in a partially internally wetted porous medium is a sum of the gas- and liquid-phase contributions

$$\bar{r} = w r_{\mathrm{l}} + (1 - w) r_{\mathrm{g}} \tag{5}$$

where $w = A_{\mathrm{wet}}/A_{\mathrm{tot}}$ is the fraction of internal surface area covered by the liquid-phase; w follows directly from the distribution of liquid- and gas-phases inside the pore space of the catalyst support. At equilibrium, two conditions must be satisfied simultaneously by all liquid–gas menisci in the pore space: (i) a contact angle ϑ must hold at all three-phase contact lines, and

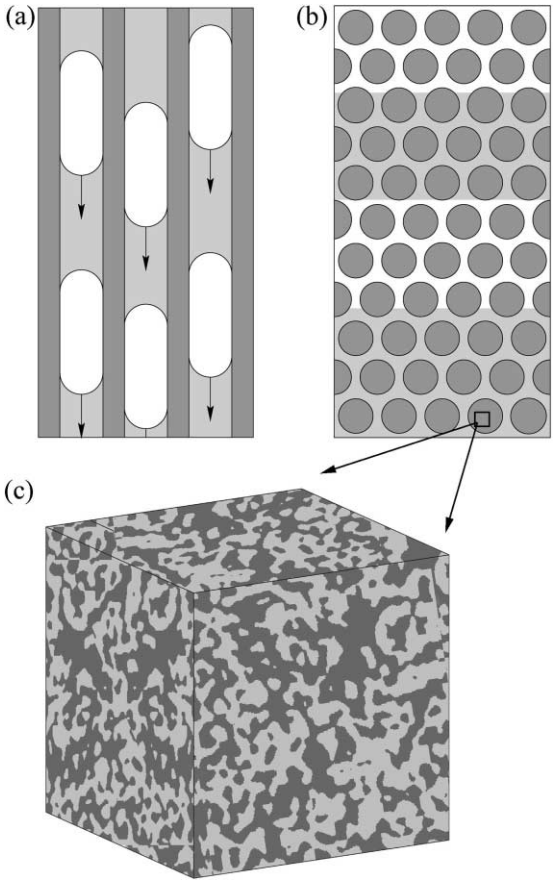

Fig. 1. (a) Periodically wetted monolith. (b) Packed bed: solid-phase is black, liquid-phase gray, and gas-phase white. (c) Liquid-saturated volume element of a porous solid (unit cell for simulations).

(ii) the curvature of all gas–liquid phase boundaries must satisfy the Young–Laplace equation

$$\Delta P = P_{\mathrm{g}} - P_{\mathrm{l}} = \sigma \left(\frac{1}{r_1} + \frac{1}{r_2} \right) \tag{6}$$

where σ is the liquid–gas interfacial tension, r_1 and r_2 are the interface curvature radii in two orthogonal directions perpendicular to the liquid–gas normal vector (by convention, r is positive for convex interfaces and negative for concave ones), and P_{g} and P_{l} are the pressures in the gas and liquid phase, respectively. It is assumed that the gas as well as the liquid phase each forms a single percolation cluster, thus P_{l} and P_{g} are identical for all (even disconnected) menisci.

When an initially dry catalyst particle (i.e., filled by gaseous component H) is externally wetted by a liquid mixture of E and A, the liquid starts to fill the internal pore space of the particle; the capillary suction continues until the pressure of the gas confined in the core of the particle offsets the capillary pressure of the invading liquid. At the same time, the reaction proceeds both in the gaseous and in the liquid phase, depleting the reactants, H and E. The gas–liquid interface in the pore space can generally continue to move, both further into the particle and back out, depending on the pressure of the gaseous core. The total change of moles Δn of the reaction is negative, thus P_{g} decreases with conversion, ceteris paribus; on the other hand, the reaction is exothermic, so the liquid can be pushed out of the particle by an expanding gas. The goal of the simulations presented here is to assess quantitatively these phenomena and the effect of selected parameters such as the liquid–solid contact angle, the mean pore diameter or the length of the wetting period on the mean reaction rate.

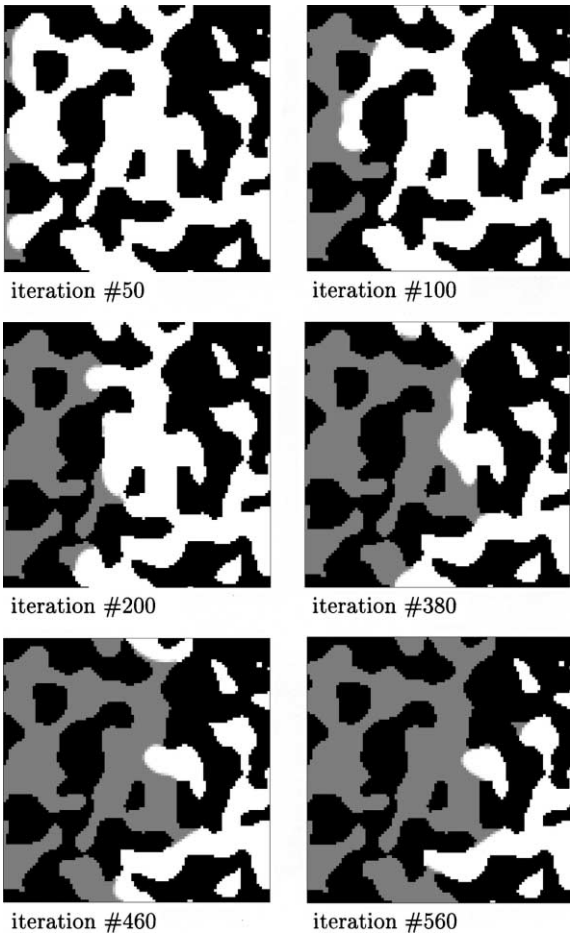

Fig. 2. Internal wetting of a slab of a porous medium. The images represent cross-section through a 3D sample; the solid phase is black, liquid phase gray, and gas-phase white. Periodic boundary conditions are applied in y and z directions, bulk liquid is on the left and bulk gas on the right in the x direction.

3. Computation procedure

A slab of a binary-encoded porous medium (cf. Fig. 1c) represents a unit cell for the simulations (the unit cell in a mesoscale simulation corresponds to a volume element ∂V of an effective medium in a macroscale simulation); it is formed by $N_x \times N_y \times N_z$ elementary cubes, periodic boundary conditions are applied in the y and z directions, bulk liquid phase is on the left and a solid wall on the right in the x direction. A Gaussian-correlated medium with correlation length $L_{\mathrm{c}} = 6$ and porosity $\varepsilon = 0.5$ was chosen as a model porous medium for the simulations [12]. For finding the equilibrium position of a liquid–gas interface in the pore space, given the gas and liquid pressures P_{g} and P_{l}, respectively, a contact angle ϑ, surface tension σ and the size of the elementary cube **a**, an algorithm for the tracking of interfaces propagating in 3D porous media with curvature-dependent velocity was used [7]. A liquid meniscus invading a small sample of a porous medium towards an equilibrium configuration is shown in Fig. 2. In a general

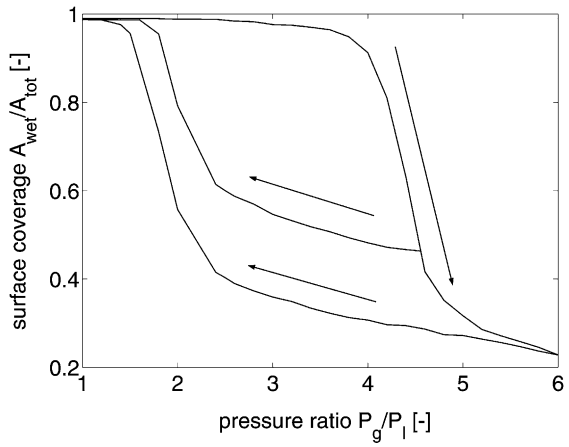

Fig. 3. Wetting hysteresis; multiple equilibrium positions of a gas–liquid interface can establish in a porous medium for the same pressure ratio, depending on the initial conditions (data for $\sigma' = 4.0$, $\vartheta = 35^\circ$, Gaussian-correlated medium with $L_c = 6$ and $\varepsilon = 0.5$, $N_x = N_y = 200$, $N_z = 50$).

3D porous medium, there can be multiple gas–liquid distributions that satisfy the equilibrium conditions (contact angle and interface curvature); the asymptotic distribution then depends on the initial conditions. Such wetting hysteresis is shown in Fig. 3, where equilibrium points obtained from an initially fully wetted medium are plotted on the upper branch of the hysteresis loop and those obtained from an initially dry medium form the lower branch. A "secondary" hysteresis curve is also shown, demonstrating that there can be a number of intermediate equilibrium configurations apart from the main hysteresis loop.

Let $f : \mathcal{P} \to \langle 0; 1\rangle$ be the fraction of an elementary cube filled by the liquid-phase, where $\mathcal{P}$ is a set of all discretization elements belonging to the pore space. Three phenomena that influence the vapor–liquid configuration in the pore space occur simultaneously: capillary flow, phase transition (evaporation/condensation), and chemical reaction. In the present work, we assume the characteristic times of the former two to be small relative to that of the latter one, thus the simulation proceeds according to the following scheme (for an isothermal case, wetting half-period):

1. Input of an encoded porous medium and the values of physico-chemical and numerical parameters; set initial conditions $t = 0\,\mathrm{s}$, $f(\mathcal{P}) = 0$ (dry particle), $T = T_0 = 298\,\mathrm{K}$, $V_g = V_0 = \sum_{\mathcal{P}} a^3\,\mathrm{m}^3$, $V_l = 0\,\mathrm{m}^3$, $P_g = P_l = P_0 = 10^5\,\mathrm{Pa}$, $p_A = p_E = 0\,\mathrm{Pa}$, $p_H = P_g$, $n_i = p_i\,V_g/(RT)$ mol, $y_i = p_i/P_g$ and $x_i = 0$.
2. Given an "old" phase distribution f and the gas-phase pressure P_g, determine a new equilibrium distribution which satisfies the contact angle ϑ and interface curvature according to the Young–Laplace equation; analyze this new f and calculate V_l, V_g and $w = A_{wet}/A_{tot}$; set $\Delta V_l = V_l - V_l^{old}$.
3. If $\Delta V_l > 0$ set $\Delta n = \Delta V_l/\bar{V}_m$, $n_E = n_E + x_E^0 \Delta n$ and $n_A = n_A + (1 - x_E^0)\Delta n$; if $\Delta V_l < 0$ set $\Delta n = -\Delta V_l/\bar{V}_m^0$, $n_E = n_E - x_E \Delta n$, $n_A = n_A - x_A \Delta n$ and $n_H = n_H - x_H \Delta n$, where $\bar{V}_m(T)$ is the mean molar volume of the liquid.
4. Determine a new equilibrium phase composition as the solution of a "flash" problem $x_i = n_i/(n_l + K_i V_g/(RT))$, $p_i = K_i x_i$ and $y_i = p_i/\sum_i p_i$, $i = A, E, H$, where K_H, $K_A = p_A^0(T)$, and $K_E = p_E^0(T)$ are equilibrium partitioning coefficients, $n_l = V_l/\bar{V}_m$, $n_g = (n_A + n_E + n_H) - n_l$, and $P_g = n_g RT/V_g$.
5. Update composition (chemical reaction) $n_i = n_i + \alpha_i\,\bar{r}\,\mathrm{d}t$, where $\alpha_A = +1$, $\alpha_E = -1$, and $\alpha_H = -1$ are stoichiometric coefficients, and the reaction rates are $r_g = r_g(T, P_g, y_E, y_H)$, $r_l = r_l(T, x_E, x_H)$, and $\bar{r} = (w r_l + (1 - w) r_g) m_s$, where $m_s = N_x\,N_y\,N_z\,a^3\,\varrho_s$.
6. Update gas-phase pressure $P_g = n_g RT/V_g$, using "new" $n_g = (n_A + n_E + n_H) - n_l$, where "pre-reaction" n_l is used, since we assume the molar volume of the liquid-phase to be independent of the composition.
7. Set $t = t + \mathrm{d}t$; if $t < \tau$, go to step 3.
8. Calculate the mean relative reaction rate η; output of the results.

Parameters that remain to be specified are the "feed" liquid-phase composition $x_E^0 = 0.2$, the contact angle ϑ which was varied between 10 and 45°, and the dimensionless capillary pressure parameter defined as

$$\sigma' \equiv \frac{\sigma}{P_l a} \tag{7}$$

which was varied from 0.2 to 5.0. The size of the elementary cube was taken as $a = 1\,\mu\mathrm{m}$, corresponding (after the multiplication by the correlation length

L_c) to typical macropore diameters of the charcoal extrudate considered. The solid-phase density is $\varrho_s = 2.267\,\mathrm{g/cm^3}$ (molar volume $V_{m,s} = 5.29\,\mathrm{cm^3/mol}$); the liquid-phase molar volume corresponding to inlet conditions (T_0, x_E^0) is $\bar{V}_m^0 = 177\,\mathrm{cm^3/mol}$.

In the non-isothermal (adiabatic) case, an enthalpy balance of the unit cell has to be considered together with the mass balance. The temperature of the unit cell is updated after the capillary flow step, the phase change step, and the reaction step. Let $\Delta_{ev}\bar{H} = \sum_i x_i \Delta_{ev} H_i$ and $\Delta_r H$ be the evaporation and reaction enthalpies, respectively, and c_s, $\bar{c}_l = \sum_i x_i c_{l,i}$, and $\bar{c}_g = \sum_i y_i c_{g,i}$ be the molar heat capacities of the solid, liquid, and vapor phases, respectively. (Standard correlations were used, yielding for the inlet conditions $\bar{c}_l = 150.2\,\mathrm{J\,K^{-1}\,mol^{-1}}$ and $\bar{c}_g = 28.88\,\mathrm{J\,K^{-1}\,mol^{-1}}$, and for the solid $c_s = 8.527\,\mathrm{J\,K^{-1}\,mol^{-1}}$.) The reaction enthalpy at 298 K is $\Delta_r H = -114.11\,\mathrm{kJ/mol}$; the heat of evaporation of the inlet mixture (20% of E in A) at 298 K is $\Delta_{ev}\bar{H} = 30.2\,\mathrm{kJ/mol}$. After the capillary flow step, the first part of the enthalpy balance is included — step 3b: if $\Delta V_l < 0$, the temperature does not change, and if $\Delta V_l > 0$, the new temperature is given by $T = (T^{old}(c_s n_s + \bar{c}_l n_l + \bar{c}_g n_g) + T_0 c_l^0 \Delta n)/(c_s n_s + \bar{c}_l(n_l + \Delta n) + \bar{c}_g n_g)$, $n_s = \varepsilon N_x N_y N_z a^3 / V_{m,s}$. After the condensation/evaporation step, the second part of the enthalpy balance is added — step 4b: $T = T^{old} + \sum_i (-\Delta_{ev} H_i)\Delta n_{g,i}/(c_s n_s + \bar{c}_l n_l + \bar{c}_g n_g)$. The final part of the enthalpy balance accounts for the released reaction heat — step 5b: $T = T^{old} + (-\Delta_r H)\bar{r}\,dt/(c_s n_s + \bar{c}_l n_l + \bar{c}_g n_g)$.

4. Results and discussion

For a quantitative evaluation of the actual reaction rate in a partially wetted particle, let us define the mean relative reaction rate

$$\eta(\tau) = \frac{1}{\tau}\int_0^\tau \frac{\bar{r}(t)}{r_0}\,dt \tag{8}$$

where τ is the length of the wetting sub-period and r_0 is the reaction rate at a reference state, which we choose as $w = 0$ (dry particle), $T = T_0$, $P_g = P_0$, $p_E = p_E^0(T_0)\,x_E^0$, and $p_H = P_g - p_E$. The dependence of η on the length of the wetting sub-period is plotted in Fig. 4 for an isothermal case, $T = 298$ K. The

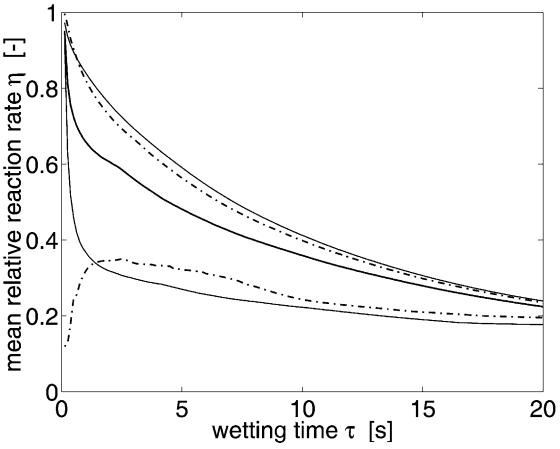

Fig. 4. Dependence of the mean relative reaction rate η on the wetting sub-period τ in an isothermal system. Parameters: $\vartheta = 30°$ and $\sigma' = 1.0$ (thick full line), $\sigma' = 0.2$ (top full line), $\sigma' = 5.0$ (bottom full line); $\sigma' = 1.0$ and $\vartheta = 15°$ (bottom dashed line), $\vartheta = 45°$ (top dashed line). Porous medium properties are the same as in Fig. 3.

dependence of $\eta(\tau)$ on two "wetting" parameters — the contact angle ϑ and the dimensionless capillary pressure σ' — was investigated. Higher values of σ' mean greater driving force for the capillary flow into the pore space, thus higher fraction of pore space filling by the condensed phase is achieved faster, and η drops correspondingly (cf. the bottom full line from Fig. 4), since in the liquid-phase, the reaction is slower than in the gas-phase. However, as the reactants (above all, H which is in a stoichiometric shortage) are depleted at a slower rate than in the case of a lower degree of internal wetting, the dependence of η on τ levels off after the initial sharp decrease and converges toward the same asymptotic value as in the case of smaller σ'.

A very interesting phenomenon was observed when investigating the influence of the catalyst support wettability by the liquid-phase (i.e., the contact angle ϑ) on $\eta(\tau)$. For smaller values of the contact angle, a qualitative change in behavior occurs, whereby the functional dependence of η on τ is not monotonously decreasing from $\eta = 1$ for $\tau = 0$, but starts from a low value, then goes through a flat maximum, and finally converges to the asymptotic value. This behavior can be attributed to the fact that due to very small contact angle (high wettability), spreading of a liquid film on the solid surface occurs initially, thus the slower liquid-phase kinetics applies and the gaseous reactant

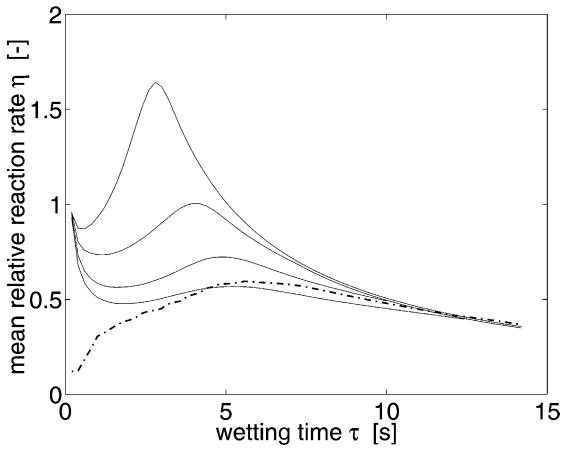

Fig. 5. Dependence of the mean relative reaction rate η on the wetting sub-period τ in an adiabatic system. Parameters: $\vartheta = 30^\circ$ and $\sigma' = 1.0$–4.0 (full lines, top to bottom); $\sigma' = 1.0$ and $\vartheta = 15^\circ$ (dashed line). Porous medium properties are the same as in Fig. 3.

H is depleted over a longer period of time at a slower, almost constant rate (cf. the bottom dashed line from Fig. 4). This has important implications for the selection of catalyst supports; new operating regimes might be obtained in a highly wettable support with relatively large mean macropore diameter, in which spreading of a liquid film instead of pore clogging by the bulk liquid would occur upon external wetting. Such operation regime is a pore-scale analogue of Taylor flow of a gas bubble in a monolith channel.

Simulations in an adiabatic unit cell were performed next; selected results are summarized in Fig. 5. The full lines show the dependence of η on τ, parametrized by the dimensionless capillary pressure σ'. For smaller values of σ' (i.e., either small surface tension or large mean pore diameter), the driving force for liquid imbibition into the porous medium is low, thus the fraction of internal surface wetted by the liquid-phase is small initially when the reactant concentration is the highest and the reaction can proceed at a fast rate (gas-phase kinetics). The generated heat causes a further increase of the reaction rate via the temperature-dependence of the rate constant. The rate of capillary suction is then slowed down (or even reversed) by an increase in the gas-phase pressure, caused by a rise of temperature. As these events form a positive feedback sequence, one can observe a relatively high parametric sensitivity with respect to σ' (cf. the peak on the uppermost solid line, which corresponds to $\sigma' = 1.0$). Practically, this means that insufficient internal wetting of the catalyst particle can lead to local overheating (similar overheating behavior has been observed experimentally in the case of incomplete external wetting).

5. Conclusion

Software enabling pore-scale simulation of simultaneous chemical reaction, phase equilibrium, and capillary flow in reconstructed porous media has been developed. It can be used for quantitative analysis of the effect of catalyst support pore structure and various physico-chemical parameters on the performance (mean reaction rate, thermal stability) of multi-phase catalytic processes and serve not only for direct simulation, but also for the estimation of experimentally directly unmeasurable quantities such as the degree of internal wetting.

Acknowledgements

Financial support from Project VS 96073 (Czech Ministry of Education), Grant 104/99/1408 (Czech Grant Agency), and Bourse du Gouvernement Français No. 11874, is gratefully acknowledged.

References

[1] M. Deem, AIChE J. 44 (1998) 2569.
[2] B. Andersson, S. Irandoust, A. Cybulski, in: Structured Catalysts and Reactors, Marcel Dekker, New York, 1998, p. 267.
[3] S. Sundaresan, AIChE J. 46 (2000) 1102.
[4] P.M. Adler, J.-F. Thovert, Appl. Mech. Rev. 51 (1998) 537.
[5] R. Lange, R. Gutsche, J. Hanika, Chem. Eng. Sci. 54 (1999) 2569.
[6] D.N. Jaguste, S.K. Bhatia, AIChE J. 37 (1991) 650.
[7] F. Štěpánek, P.M. Adler, M. Marek, AIChE J. 45 (1999) 1901.
[8] M.P. Harold, in: Computer-Aided Design of Catalysts, Marcel Dekker, New York, 1993, p. 391.
[9] J. Růžička, J. Hanika, Catal. Today 20 (1994) 467.
[10] C. Kouris, S. Neophytides, C.G. Vayenas, J. Tsamopoulos, Chem. Eng. Sci. 53 (1998) 3129.
[11] J. Krausová, M.Sc. Thesis, Institute of Chemical Technology, Prague, 1973.
[12] F. Štěpánek, P.M. Adler, M. Kubíček, M. Marek, in: Computer-Aided Chemical Engineering, Vol. 8, Elsevier, Amsterdam, 2000, p. 667.